Editors' Suggestion    Featured in Physics

# Nuclear Charge Radius of $^{26m}$Al and Its Implication for $V_{ud}$ in the Quark Mixing Matrix

P. Plattner,[1,2,3,*] E. Wood,[4] L. Al Ayoubi,[5] O. Beliuskina,[5] M. L. Bissell,[6,1] K. Blaum,[3] P. Campbell,[6] B. Cheal,[4]
R. P. de Groote,[5,‡] C. S. Devlin,[4] T. Eronen,[5] L. Filippin,[7] R. F. Garcia Ruiz,[1,8] Z. Ge,[5] S. Geldhof,[9] W. Gins,[5]
M. Godefroid,[7] H. Heylen,[1,3] M. Hukkanen,[5] P. Imgram,[10] A. Jaries,[5] A. Jokinen,[5] A. Kanellakopoulos,[9]
A. Kankainen,[5] S. Kaufmann,[10] K. König,[10] Á. Koszorús,[4,9,‡] S. Kujanpää,[5] S. Lechner,[1] S. Malbrunot-Ettenauer,[1,11,†]
P. Müller,[10] R. Mathieson,[4] I. Moore,[5] W. Nörtershäuser,[10] D. Nesterenko,[5] R. Neugart,[3,12]
G. Neyens,[1,9] A. Ortiz-Cortes,[5] H. Penttilä,[5] I. Pohjalainen,[5] A. Raggio,[5] M. Reponen,[5] S. Rinta-Antila,[5]
L. V. Rodríguez,[3,1,13] J. Romero,[5] R. Sánchez,[14] F. Sommer,[10] M. Stryjczyk,[5] V. Virtanen,[5] L. Xie,[6]
Z. Y. Xu,[9] X. F. Yang,[9,15] and D. T. Yordanov[13]

[1]*ISOLDE, CERN Experimental Physics Department, Geneva 23, 1211 Genevè, Switzerland*
[2]*Universität Innsbruck, Innrain 52, 6020 Innsbruck, Austria*
[3]*Max-Planck-Institut für Kernphysik, Saupfercheckweg 1, 69117 Heidelberg, Germany*
[4]*Department of Physics, University of Liverpool, Liverpool L69 7ZE, United Kingdom*
[5]*Department of Physics, University of Jyväskylä, P.O. Box 35 FI-40014, Jyväskylä, Finland*
[6]*Department of Physics and Astronomy, University of Manchester, Oxford Road, Manchester M13 9PL, United Kingdom*
[7]*Spectroscopy, Quantum Chemistry and Atmospheric Remote Sensing (SQUARES),*
*Université libre de Bruxelles, 1050 Brussels, Belgium*
[8]*Massachusetts Institute of Technology, 77 Massachusetts Ave, Cambridge, Massachusetts 02139, USA*
[9]*Instituut voor Kern- en Stralingsfysica, KU Leuven, 3001 Leuven, Belgium*
[10]*Institut für Kernphysik, Technische Universität Darmstadt, Schlossgartenstraße 9, 64289 Darmstadt, Germany*
[11]*TRIUMF, 4004 Wesbrook Mall, Vancouver, British Columbia V6T 2A3, Canada*
[12]*Institut für Kernchemie, Universität Mainz, Fritz-Straßmann-Weg 2, 55128 Mainz, Germany*
[13]*IJCLab, CNRS/IN2P3, Université Paris-Saclay, 91400 Orsay, France*
[14]*GSI Helmholtzzentrum für Schwerionenforschung, Planckstraße 1, 64291 Darmstadt, Germany*
[15]*School of Physics and State Key Laboratory of Nuclear Physics and Technology, Peking University,*
*209 Chengfu Road, 100871 Beijing, China*

Collinear laser spectroscopy was performed on the isomer of the aluminium isotope $^{26m}$Al. The measured isotope shift to $^{27}$Al in the $3s^2 3p\,^2P^\circ_{3/2} \rightarrow 3s^2 4s\,^2S_{1/2}$ atomic transition enabled the first experimental determination of the nuclear charge radius of $^{26m}$Al, resulting in $R_c = 3.130(15)$ fm. This differs by 4.5 standard deviations from the extrapolated value used to calculate the isospin-symmetry breaking corrections in the superallowed $\beta$ decay of $^{26m}$Al. Its corrected $\mathcal{F}t$ value, important for the estimation of $V_{ud}$ in the Cabibbo-Kobayashi-Maskawa matrix, is thus shifted by 1 standard deviation to 3071.4(1.0) s.

*Introduction.*—The Cabibbo-Kobayashi-Maskawa (CKM) matrix is a central cornerstone in the formulation of the standard model of particle physics. It connects the quarks' mass with weak eigenstates and, thus, characterizes the strength of quark-flavor mixing through the weak interaction. The first element in the top row of the matrix, $V_{ud}$, manifests in the $\beta$ decay of pions, neutrons, or radioactive nuclei. While individual entries of the quark mixing matrix

cannot be predicted within the standard model, the CKM matrix is required to be unitary—a tenet which is the subject of intense experimental scrutiny.

In recent years, the unitary test of the top-row elements:

$$|V_{ud}|^2 + |V_{us}|^2 + |V_{ub}|^2 = 1 - \Delta_{\mathrm{CKM}}$$

has received significant attention. The unitarity of the CKM matrix demands the residual $\Delta_{\mathrm{CKM}}$ to vanish. However, recent advances in the theoretical description of (inner) radiative corrections [1–6] to $\beta$ decays resulted in a notable shift in $V_{ud}$ and, thus, to a tension with respect to CKM unitarity. Following recommended values by the Particle Data Group [7], $\Delta_{\mathrm{CKM}} = 15(7) \times 10^{-4}$ hints at a $\approx 2\sigma$

deviation from unitarity although this discrepancy could be as large as $5.5\sigma$, depending on which calculation of (nuclear-structure dependent [2,8–10] and universal [1–3,6]) radiative corrections are used in the determination of $V_{ud}$ and which decay is considered to obtain $V_{us}$ [7,11–16].

At present, superallowed $0^+ \to 0^+$ nuclear $\beta$ decays remain the most precise way to access $V_{ud}$ [10]. For these cases, the experimentally measured $ft$ value, characterizing a $\beta$ decay, can be related to a corrected $\mathcal{F}t$ value:

$$\mathcal{F}t = ft \cdot (1 + \delta'_R)(1 + \delta_{NS} - \delta_C), \qquad (1)$$

where $\delta'_R$ and $\delta_{NS}$ constitute the transition-dependent contributions to the radiative corrections while $\delta_C$ are the isospin-symmetry breaking (ISB) corrections. According to the conserved vector-current hypotheses, the $\mathcal{F}t$ values should be identical for all superallowed $\beta$ decays. When averaged over all 15 precision cases, they serve to extract $V_{ud}$.

While the experimental dataset on $ft$ values of superallowed $\beta$ decays robustly builds on 222 individual measurements [10], theoretical corrections are under scrutiny. As part of this process, the uncertainties in the nuclear-structure dependent radiative corrections $\delta_{NS}$ have recently been inflated by a factor of $\approx 2.6$ [10]. Moreover, the ISB corrections $\delta_C$, which are also nuclear-structure dependent, remain an ongoing focus of research which has stimulated new theoretical calculations [17–20] as well as experimental benchmarks [21–26].

For the determination of $V_{ud}$, $^{26m}$Al is of particular importance. The nuclear-structure dependent corrections, $\delta_{NS} - \delta_C$, in $^{26m}$Al are the smallest in size among all superallowed $\beta$ emitters [10]. The same holds true for the combined experimental and theoretical uncertainties in the $\mathcal{F}t$ value of $^{26m}$Al [10]. Its extraordinary precision is thus almost on par with all other precision cases combined. In times of tension with CKM unitary and rigorous examination of all involved theoretical corrections, it is, therefore, unsettling that one critical input parameter for the calculation of $\delta_C$, i.e., the nuclear charge radius, is in the case of $^{26m}$Al, based on an extrapolated but experimentally unknown value [27,28].

In this Letter, we report on isotope-shift measurements obtained via collinear laser spectroscopy (CLS) that puts the nuclear charge radius of $^{26m}$Al on solid experimental footings. Implications for its $\mathcal{F}t$ value and, thus, $V_{ud}$ are discussed.

*Experiment.*—Two independent experiments were performed, one at the COLLAPS beamline [29] at ISOLDE-CERN [30] and the other at the IGISOL CLS beamline [31] in Jyväskylä-Finland. Details of the campaign on aluminium isotopes at COLLAPS are described in Ref. [32]. In short, radioactive aluminium atoms were synthesised by bombarding a uranium carbide target with 1.4-GeV protons from CERN's PS booster. Once released from the production target, the Al$^+$ ion beam was formed via resonant laser ionization [33], subsequent electrostatic acceleration to 30 keV, and final mass selection via ISOLDE's magnetic high-resolution separator [34].

At IGISOL [35], the radionuclides of interest were produced in $^{27}$Al(p, d) reactions at 25-MeV proton energy. After their release from a thin foil target and extraction from the He-gas filled gas cell, the Al ions were guided towards the high vacuum region of the mass separator via a sextupole ion guide, accelerated to 30 keV and mass separated by a 55° dipole magnet.

In both experiments, the ions were stopped, cooled, and accumulated in a buffer-gas filled radio-frequency-quadrupole cooler buncher [36,37] before they were delivered in 30-keV ion bunches to the respective CLS beamline. There, the ion beam was spatially superimposed with the laser beam in collinear (COLLAPS) or anticollinear (IGISOL) fashion. The ions' velocity was adjusted by a Doppler-tuning voltage applied before the neutralization in a charge exchange cell filled with sodium vapor. In this manner, the laser frequency experienced in the rest frame of the neutral Al atoms could be scanned via Doppler tuning. Once on resonance with the selected transition, fluorescence was detected using a series of photomultiplier tubes and their associated lens systems which surrounded the laser-atom interaction region [38,39].

In both campaigns, the main spectroscopic transition was from the atomic $3s^2 3p\ ^2P^\circ_{3/2} \to 3s^2 4s\ ^2S_{1/2}$ level at $25\,235.695$ cm$^{-1}$. Suitable laser light was provided by a continuous wave titanium:sapphire ring laser (Sirah Matisse 2) set to an output wavelength of 792 nm. The resulting laser light was frequency doubled using an external cavity frequency doubler (Wavetrain 2), after which the laser beam with a few milliwatts in power was sent through the experimental beamlines. To compensate for long-term drifts in both experiments, the fundamental laser was locked in wavelength to a HighFinesse WSU-10 wave meter which was regularly calibrated to a frequency-stabilized HeNe laser.

In addition to the low-lying $^{26m}$Al isomer with a half-life of $T_{1/2} = 6.34602(54)$ s [10], the long-lived ground state $^{26}$Al $[T_{1/2} = 7.14(24) \times 10^5$ y [40]] was also present in the radioactive ion beams, although in different relative intensities that reflected the distinct production methods at ISOLDE and IGISOL. Examples of the obtained resonance spectra of $^{26,26m}$Al are shown in Fig. 1. Because of the dense hyperfine structure of $^{26}$Al (nuclear spin $I = 5$) and the small isomer shift, the single peak associated with $^{26m}$Al ($I = 0$) could not be resolved from the strongest transition in $^{26}$Al. In order to unambiguously demonstrate the presence of the isomer, the transition $3s^2 3p\ ^2P^\circ_{1/2} \to 3s^2 3d\ ^2D_{3/2}$ at 308 nm was additionally utilized during the campaign at IGISOL. As visible in the inset of Fig. 1(a), by exploiting the latter transition the multiplets in the
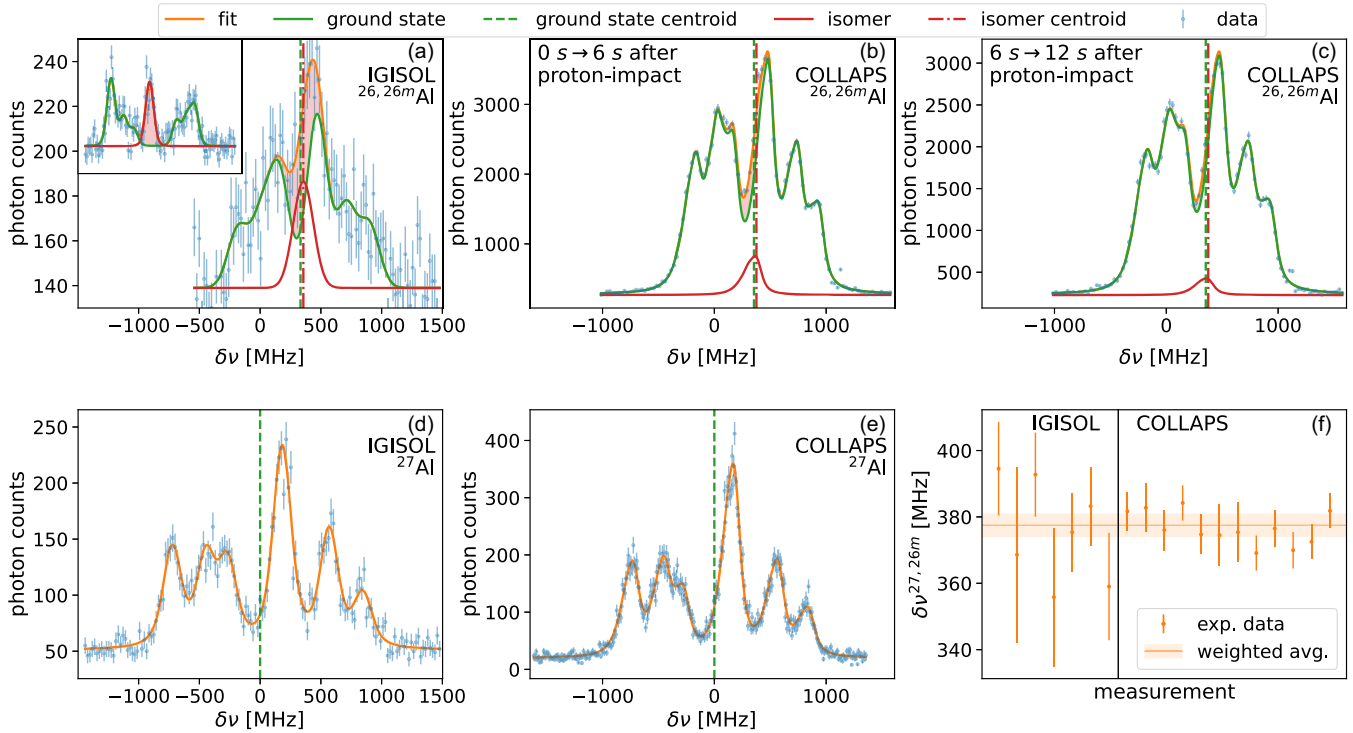
FIG. 1. (a) Example of a resonance spectrum of the main spectroscopic transition $3s^2 3p\ ^2P^\circ_{3/2} \to 3s^2 4s\ ^2S_{1/2}$ obtained in the CLS measurements of $^{26,26m}$Al at IGISOL. The inset demonstrates the isomer's presence (red) due to well separated ground and isomer states in the $3s^2 3p\ ^2P^\circ_{1/2} \to 3s^2 3d\ ^2D_{3/2}$ transition. (b),(c) The spectra of $^{26,26m}$Al in the main transition at COLLAPS. Ions have been extracted 0 (b) and 6 s (c) after the proton impact on the ISOLDE target, demonstrating the isomer's presence due to the decrease in intensity consistent with the isomer's half-life. (d),(e) Examples of resonance spectra of the $^{27}$Al references studied using the main transition at IGISOL (d) and COLLAPS (e). (f) Extracted isotope shifts (points) and the resulting weighted average (a horizontal line), including systematic uncertainties.

hyperfine spectrum of $^{26}$Al were well separated (green line) and offered unobstructed access to the resonance peak of $^{26m}$Al (red). However, due to state mixing with a second close-lying atomic state ($\Delta E \approx 0.17$ meV), this transition is inadequate for the determination of nuclear charge radii [41].

To confirm the presence of the isomer in the ISOLDE beam, we took advantage of the pulsed time structure of the proton beam and the long release time of Al from the ISOLDE target. In a set of dedicated measurements, subsequent proton pulses were separated in time by at least 12 s corresponding to approximately two half-lives of $^{26m}$Al. The recorded fluorescence data was divided into two sets which were measured up to 6 s and between 6 and 12 s after the proton impact, see Figs. 1(b) and 1(c), respectively. The resonances' intensities for the long-lived ground state (green) changed only slightly between these two datasets, likely because of a small time dependence in the Al release. The much stronger decrease in isomer intensity (red) between the first and second 6 s of data taking was consistent with the isomer's half-life when each is normalized to the corresponding ground-state intensity.

Direct comparison of the spectra shows a higher overall rate and thus better statistics for the COLLAPS data set. This statement holds true for both measurements of $^{26,26m}$Al as well as stable $^{27}$Al, see Figs. 1(d) and 1(e), which were interleaved with online data as reference measurements. On the other hand, the data from IGISOL benefits from a more favorable isomer-to-ground state ratio, compare Figs. 1(a) and 1(b). The complementarity of the COLLAPS and IGISOL datasets in terms of high statistics versus better isomer-ground state ratio was further strengthened by their distinct control and evaluation of systematic uncertainties. Most importantly, the determination of the ion-acceleration voltage at COLLAPS was achieved by a high-precision voltage divider. At IGISOL, it was calibrated by CLS measurements of stable magnesium (Mg) ions with respect to their precisely known isotope shifts.

*Analysis and results.*—The measured resonance spectra of $^{26,26m,27}$Al were fitted to the theoretical model of the hyperfine spectra using the SATLAS package [42]. To constrain the fit in the present work, the ratio of the hyperfine parameters $A(P_{3/2})/A(S_{1/2})$ was fixed to the precise value of 4.5701(14), obtained in previous work on Al isotopes at COLLAPS [32]. However, this constraint

was not applied to the present $^{27}$Al part of the COLLAPS analysis as the analyzed spectra were a subset of the measurements examined in Ref. [32].

For $^{26,26m}$Al, a model of the $I = 5$ ground state and one of the $I = 0$ isomeric state were superimposed. Within each experimental campaign, all $^{26,26m}$Al resonance spectra were fitted simultaneously with the same, shared hyperfine parameters as long as a parameter was not otherwise constrained, see above. Similarly, the isomer shift between ground and isomeric state in $^{26}$Al was implemented as a shared fit parameter across a campaign's entire dataset. The isomer centroid $\nu_0^{26m}$ itself was freely varied for each individual spectrum. For the determination of $\nu_0^{26m}$, the Doppler-tuning voltage was converted into frequency based on the isomer's ionic mass. It was verified in fits of simulated spectra that this approach led to accurate results despite the peak overlap with the resonance spectrum of the ground state.

Voigt profiles were chosen for the line shapes of individual resonance peaks with no intensity constraints in the ground state. The Lorentzian and Gaussian widths were shared between ground state and isomer peaks within each individual spectrum but not shared overall. Because of inelastic collisions in the charge-exchange cell [38,43,44], four equidistant side peaks were considered in the analysis of the COLLAPS data [32]. The energy offset of these sidepeaks was determined empirically and the relative intensities were constrained by Poisson's law. Because of lower statistics, the IGISOL data were found to be insensitive to the inclusion of these sidepeaks, thus, they were not considered in the analysis.

Each spectrum of $^{26,26m}$Al was measured in sequence with an independent $^{27}$Al reference measurement. The isotope shift $\delta\nu^{27,26m} = \nu_0^{26m} - \nu_0^{27}$ of each measurement pair was calculated from the frequency centroid $\nu_0^{26m}$ of $^{26m}$Al with respect to the frequency centroid $\nu_0^{27}$ of the closest $^{27}$Al reference measurement. The results of all individual $\delta\nu^{27,26m}$ determinations are shown in Fig. 1(f). Weighted averages in $\delta\nu^{27,26m}$ are calculated separately for the COLLAPS and IGISOL datasets, see Table I.

Systematic uncertainties in CLS for measurements of isotope shifts are well understood [45–48] and are dominated by the imperfect knowledge of the beam energy. The acceleration voltage from the cooler-buncher at IGISOL was calibrated by matching measured isotope shifts in the D1 and D2 lines for singly charged ions of stable magnesium isotopes to their precisely known literature values in Ref. [49]. The remaining uncertainty in beam energy was 1.8 eV. An additional $1 \times 10^{-4}$ relative uncertainty was assigned to the scanning voltage in the Doppler tuning. For the COLLAPS data, a $1.5 \times 10^{-4}$ relative uncertainty of the incoming ion beam energy was assigned following the specifications of the employed voltage divider (Ohmlabs KV-30A). This was combined with the

TABLE I. Measured isotope shift $\delta\nu^{27,26m}$ between $^{27}$Al and $^{26m}$Al obtained at the IGISOL facility and at COLLAPS-ISOLDE. The weighted average of the two measurements and the resulting difference in mean square charge radius $\delta\langle r_c^2 \rangle^{27,26m}$ is listed.

| | $\delta\nu^{27,26m}$ (MHz) | $\delta\langle r_c^2 \rangle^{27,26m}$ (fm$^2$) |
|---|---|---|
| COLLAPS | 376.5\{1.7\}[3.7][a] | |
| IGISOL | 379.7\{5.5\}[2.2][a] | |
| Weighted average | 377.5(3.4)[b] | 0.429(45)⟨76⟩[b] |

[a]Statistical and systematic uncertainties given in curly and square brackets, respectively.
[b]Combined statistical and systematic uncertainties in parentheses. Uncertainty from atomic physics calculations of mass and field shift from [32] in angle brackets.

uncertainties of the calibrated JRL KV10 voltage divider used to measure the scanning voltage and of the employed voltmeters (Agilent 34661A).

Since the systematic uncertainties at COLLAPS and IGISOL were fully independent, statistical and systematic uncertainties of each measurement campaign were first added in quadrature before the weighted average of both measurement results was calculated, see Table I. Our final value for the isotope shift between $^{26m}$Al and $^{27}$Al is $\delta\nu^{27,26m} = 377.5(3.4)$ MHz.

With knowledge of the isotope shift $\delta\nu^{27,26m}$ the difference in mean square nuclear charge radii $\delta\langle r^2 \rangle$ between the two isotopes could be calculated according to [50]

$$\delta\nu^{27,26m} = F\delta\langle r^2 \rangle^{27,26m} + M\frac{m_{26m} - m_{27}}{m_{27}(m_{26m} + m_e)},$$

where $m_e$ is the electron mass [51] and $m_A$ are the nuclear masses obtained when 13 electrons are subtracted from the atomic masses [52] and an excitation energy of 228.305 keV [53] is added for $^{26m}$Al. Precision atomic-physics calculations were performed in a multiconfiguration Dirac-Hartree-Fock framework to evaluate the field and mass shift factors $F$ and $M$ of the investigated atomic transition [32,54]. Combining the adopted values of $F = 76.2(2.2)$ MHz/fm$^2$ and $M = -243(4)$ GHz u with the isotope shift $\delta\nu^{27,26m}$ of the present work yields $\delta\langle r^2 \rangle_{27,26m} = 0.429(88)$ fm$^2$, see Table I. Finally, the root mean square (rms) nuclear charge radius of $^{26m}$Al can be derived:

$$R_c(^{26m}\text{Al}) \equiv \langle r^2 \rangle_{26m}^{1/2} = \sqrt{R_c(^{27}\text{Al})^2 + \delta\langle r^2 \rangle^{27,26m}}.$$

Using the previously evaluated rms charge radius of $^{27}$Al, $R_c(^{27}\text{Al}) = 3.061(6)$ fm [32], a value of $R_c(^{26m}\text{Al}) = 3.130(15)$ fm is obtained, see Table II.

*Discussion.*—Nuclear charge radii of superallowed $\beta$ emitters are essential input parameters for the calculation of

TABLE II. Summary of the rms charge radius $R_c$, the radial overlap correction $\delta_{C2}$ and the $\mathcal{F}t$ value of $^{26m}$Al, the weighted average of the 15 superallowed $\beta$ emitters $\overline{\mathcal{F}t}$ and the result of the CKM unitarity test.

| Quantity | Previous value | This Letter |
|---|---|---|
| $R_c$ | 3.040(20) fm [27] | 3.130(15) fm |
| $\delta_{C2}$ | 0.280(15)% [10] | 0.310(14)% |
| $\mathcal{F}t(^{26m}Al)$ | 3072.4(1.1) s [10] | 3071.4(1.0) s |
| $\overline{\mathcal{F}t}$ | 3072.24(1.85) s [10] | 3071.96(1.85) s |
| $\Delta_{CKM}$ | $152(70) \times 10^{-5}$ [7] | $144(70) \times 10^{-5}$ |

the ISB corrections $\delta_C$ when a nuclear shell-model approach with Woods-Saxon radial wave functions is employed [27,28]. Currently, these $\delta_C$ calculations are the only ones considered to be sufficiently reliable to evaluate $\mathcal{F}t$ values and thus $V_{ud}$ [10]. In the shell-model approach, the ISB corrections are separated into two components, $\delta_C = \delta_{C1} + \delta_{C2}$. The former is associated with the configuration mixing within the restricted shell model space while the latter, known as the radial overlap correction, is derived from a phenomenological Woods-Saxon potential and it depends on the nuclear charge radius $R_c$.

Since $R_c(^{26m}Al)$ was previously unknown, the calculation of $\delta_{C2}$ used $R_c = 3.040(20)$ fm [27], an extrapolation based on other, known nuclear charge radii. Our experimental result, $R_c(^{26m}Al) = 3.130(15)$ fm, deviates from this extrapolation by 4.5 standard deviations. This significantly impacts the radial overlap correction which is updated to $\delta_{C2} = 0.310(14)$ % [55] compared to the previous 0.280(15) % [10]. The impacts of this sizable change in $\delta_{C2}$ are summarized in Fig. 2(a) and in Table II.

Despite $^{26m}$Al being the most accurately studied superallowed $\beta$ emitter, the corrected $\mathcal{F}t$ value is shifted by almost 1 full standard deviation to 3071.4(1.0) s. Its high precision is maintained but, in terms of $R_c$ in the calculation of $\delta_C$, the value now stands on a solid experimental basis. The updated $\mathcal{F}t$ value of $^{26m}$Al also affects the $\overline{\mathcal{F}t}$ value, i.e., the weighted average over all 15 precisely studied superallowed $\beta$ emitters, which is shifted by one-half of its statistical uncertainty, see inset in Fig. 2(a). To our knowledge, this represents the largest shift in the $\overline{\mathcal{F}t}$ value since 2009, see Fig. 2(b). This is a remarkable influence of a single experimental result on a quantity which is based on more than 200 individual measurements and which is dominated in its uncertainty by theoretical corrections.

Accounting for 0.57 s, this statistical uncertainty contains all experimental as well as those theoretical errors which scatter "randomly" from one superallowed transition to another. Previously, a single systematic theoretical uncertainty of 0.36 s due to $\delta'_R$ had to be added affecting all superallowed $\beta$ emitters alike [56]. In these circumstances, the shift in the $\overline{\mathcal{F}t}$ value caused by the new charge
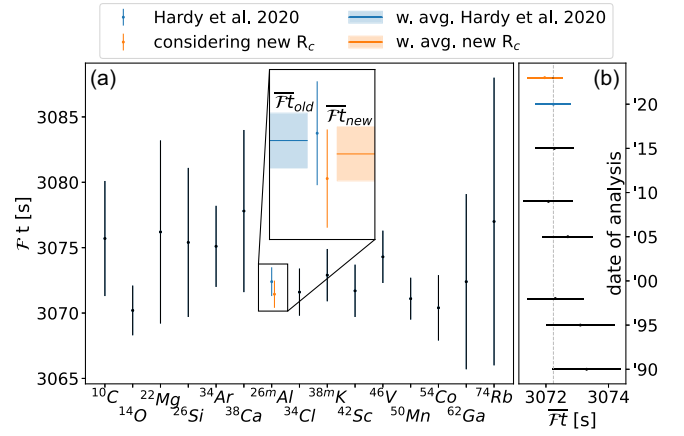


FIG. 2. (a) $\mathcal{F}t$ values of the 15 superallowed $\beta$ emitters used to determine $V_{ud}$. The values in black, taken from [10], include experimental as well as "statistical" theoretical errors. The previously determined $\mathcal{F}t$ value for $^{26m}$Al [10] (blue) is compared to the one (orange) when considering the experimental nuclear charge radius of the present work. The weighted averages for the 15 superallowed $\beta$ emitters are shown as horizontal bars in the inset (without considering additional, systematic theoretical uncertainties). (b) Evolution of the $\overline{\mathcal{F}t}$ value with statistical uncertainties in previous reviews [10,56–61] (black) compared to this Letter (orange). The vertical line to guide the eye corresponds to the value from 2020 [10].

radius of $^{26m}$Al would have corresponded to $\approx 40\%$ of its total uncertainty. In the latest survey of superallowed $\beta$ decays [10], however, a systematic theoretical uncertainty of 1.73 s in $\delta_{NS}$ was newly introduced, reflecting uncertainties due to previously unaccounted contributions to the nuclear-structure dependent radiative corrections. This represents an almost threefold increase of the theoretical error associated with $\delta_{NS}$ which now dominates the uncertainty in the $\overline{\mathcal{F}t}$ value. Considering our new charge radius of $^{26m}$Al, one thus obtains an $\overline{\mathcal{F}t}$ value of 3071.96(1.85) s.

The present work further implies a $\Delta_{CKM}$ in the unitarity test of the first row of the CKM matrix which is brought by $\approx 1/10\sigma$ closer towards unitarity. Although the magnitude of this change is too small to resolve the tension to CKM unitarity, it illustrates the importance of a comprehensive examination of all relevant ingredients to $V_{ud}$, especially theoretical corrections which involve nuclear-structure dependencies such as radiative and ISB corrections. In terms of $\delta_{C2}$, there remain seven superallowed $\beta$ emitters in which the nuclear charge radius is experimentally undetermined [62,63]. Among those, $^{10}$C and $^{14}$O are of specific interest given their sensitivity to the Fierz interference term which relates to scalar contributions in $\beta$ decays. Moreover, it has recently been proposed to constrain models of ISB corrections by new, more precise measurements of charge radii in triplets of the isobaric analog states, e.g., $^{38}$Ca-$^{38m}$K-$^{38}$Ar [20].

*Summary.*—Collinear laser spectroscopy has been performed to determine the nuclear charge radius of $^{26m}$Al, the most precisely studied superallowed $\beta$ emitter. The obtained value differs by 4.5 standard deviations from the extrapolation used in the calculation of the isospin-symmetry-breaking corrections [10,27]. This notably impacts the corrected $\mathcal{F}t$ value in $^{26m}$Al and, thus, the average of all $\mathcal{F}t$ values used in the extraction of $V_{ud}$. As demanded by the tension in CKM unitarity, this Letter contributes to the thorough examination of all nuclear-structure dependent corrections in superallowed $\beta$ decays. Stimulated by the present results, efforts to measure experimentally undetermined charge radii of other cases, for example $^{54}$Co at IGISOL-Jyväskylä, are currently ongoing.

---

[*]Corresponding author: peter.plattner@cern.ch
[†]Corresponding author: stephan.ettenauer@cern.ch
[‡]Present address: Instituut voor Kern- en Stralingsfysica, KU Leuven, 3001 Leuven, Belgium.

[1] C.-Y. Seng, M. Gorchtein, H. H. Patel, and M. J. Ramsey-Musolf, Phys. Rev. Lett. **121**, 241804 (2018).
[2] C.-Y. Seng, M. Gorchtein, and M. J. Ramsey-Musolf, Phys. Rev. D **100**, 013001 (2019).
[3] A. Czarnecki, W. J. Marciano, and A. Sirlin, Phys. Rev. D **100**, 073008 (2019).
[4] C.-Y. Seng, X. Feng, M. Gorchtein, and L.-C. Jin, Phys. Rev. D **101**, 111301(R) (2020).
[5] L. Hayen, Phys. Rev. D **103**, 113001 (2021).
[6] K. Shiells, P. G. Blunden, and W. Melnitchouk, Phys. Rev. D **104**, 033003 (2021).
[7] R. L. Workman *et al.* (Particle Data Group), Prog. Theor. Exp. Phys. **2022**, 083C01 (2022).
[8] I. Towner, Phys. Lett. B **333**, 13 (1994).
[9] M. Gorchtein, Phys. Rev. Lett. **123**, 042503 (2019).
[10] J. C. Hardy and I. S. Towner, Phys. Rev. C **102**, 045501 (2020).
[11] N. Cabibbo, E. C. Swallow, and R. Winston, Annu. Rev. Nucl. Part. Sci. **53**, 39 (2003).
[12] N. Cabibbo, E. C. Swallow, and R. Winston, Phys. Rev. Lett. **92**, 251803 (2004).
[13] F. Ambrosino *et al.*, Phys. Lett. B **632**, 76 (2006).
[14] M. Antonelli, V. Cirigliano, G. Isidori, F. Mescia, M. Moulson, H. Neufeld, E. Passemar, M. Palutan, B. Sciascia, M. Sozzi, R. Wanke, and O. P. Yushchenko, Eur. Phys. J. C **69**, 399 (2010).
[15] Y. Amhis *et al.*, Eur. Phys. J. C **81**, 226 (2021).
[16] Y. Aoki *et al.* (Flavour Lattice Averaging Group (FLAG)), Eur. Phys. J. C **82**, 869 (2022).
[17] W. Satuła, P. Baczyk, J. Dobaczewski, and M. Konieczka, Phys. Rev. C **94**, 024306 (2016).
[18] L. Xayavong and N. A. Smirnova, Phys. Rev. C **97**, 024324 (2018).
[19] M. S. Martin, S. R. Stroberg, J. D. Holt, and K. G. Leach, Phys. Rev. C **104**, 014324 (2021).
[20] C.-Y. Seng and M. Gorchtein, Phys. Lett. B **838**, 137654 (2023).
[21] D. Melconian, S. Triambak, C. Bordeanu, A. García, J. C. Hardy, V. E. Iacob, N. Nica, H. I. Park, G. Tabacaru, L. Trache, I. S. Towner, R. E. Tribble, and Y. Zhai, Phys. Rev. Lett. **107**, 182301 (2011).
[22] I. S. Towner and J. C. Hardy, Phys. Rev. C **82**, 065501 (2010).
[23] H. I. Park, J. C. Hardy, V. E. Iacob, M. Bencomo, L. Chen, V. Horvat, N. Nica, B. T. Roeder, E. Simmons, R. E. Tribble, and I. S. Towner, Phys. Rev. Lett. **112**, 102502 (2014).
[24] S. Malbrunot-Ettenauer, T. Brunner, U. Chowdhury, A. T. Gallant, V. V. Simon, M. Brodeur, A. Chaudhuri, E. Mané, M. C. Simon, C. Andreoiu, G. Audi, J. R. Crespo López-Urrutia, P. Delheij, G. Gwinner, A. Lapierre, D. Lunney, M. R. Pearson, R. Ringle, J. Ullrich, and J. Dilling, Phys. Rev. C **91**, 045504 (2015).
[25] M. Bencomo, J. C. Hardy, V. E. Iacob, H. I. Park, L. Chen, V. Horvat, N. Nica, B. T. Roeder, A. Saastamoinen, and I. S. Towner, Phys. Rev. C **100**, 015503 (2019).
[26] V. E. Iacob, J. C. Hardy, H. I. Park, M. Bencomo, L. Chen, V. Horvat, N. Nica, B. T. Roeder, A. Saastamoinen, and I. S. Towner, Phys. Rev. C **101**, 045501 (2020).
[27] I. S. Towner and J. C. Hardy, Phys. Rev. C **66**, 035501 (2002).
[28] I. S. Towner and J. C. Hardy, Phys. Rev. C **77**, 025501 (2008).
[29] R. Neugart, J. Billowes, M. L. Bissell, K. Blaum, B. Cheal, K. T. Flanagan, G. Neyens, W. Nörtershäuser, and D. T. Yordanov, J. Phys. G **44**, 064002 (2017).
[30] R. Catherall, W. Andreazza, M. Breitenfeldt, A. Dorsival, G. J. Focker, T. P. Gharsa, T. J. Giles, J.-L. Grenard,

F. Locci, P. Martins, S. Marzari, J. Schipper, A. Shornikov, and T. Stora, J. Phys. G **44**, 094002 (2017).

[31] L. J. Vormawah, M. Vilén, R. Beerwerth, P. Campbell, B. Cheal, A. Dicker, T. Eronen, S. Fritzsche, S. Geldhof, A. Jokinen, S. Kelly, I. D. Moore, M. Reponen, S. Rinta-Antila, S. O. Stock, and A. Voss, Phys. Rev. A **97**, 042504 (2018).

[32] H. Heylen *et al.*, Phys. Rev. C **103**, 014318 (2021).

[33] V. Fedosseev, K. Chrysalidis, T. D. Goodacre, B. Marsh, S. Rothe, C. Seiffert, and K. Wendt, J. Phys. G **44**, 084006 (2017).

[34] T. J. Giles, R. Catherall, V. Fedosseev, U. Georg, E. Kugler, J. Lettry, and M. Lindroos, Nucl. Instrum. Methods Phys. Res., Sect. B **204**, 497 (2003).

[35] I. D. Moore, P. Dendooven, and J. Ärje, Hyperfine Interact. **223**, 17 (2014).

[36] A. Nieminen, P. Campbell, J. Billowes, D. H. Forest, J. A. R. Griffith, J. Huikari, A. Jokinen, I. D. Moore, R. Moore, G. Tungate, and J. Äystö, Phys. Rev. Lett. **88**, 094801 (2002).

[37] H. Frånberg *et al.*, Nucl. Instrum. Methods Phys. Res., Sect. B **266**, 4502 (2008).

[38] K. Kreim, M. Bissell, J. Papuga, K. Blaum, M. De Rydt, R. García Ruíz, S. Goriely, H. Heylen, M. Kowalska, R. Neugart, G. Neyens, W. Nörtershäuser, M. Rajabali, R. Sánchez Alarcón, H. Stroke, and D. Yordanov, Phys. Lett. B **731**, 97 (2014).

[39] R. P. de Groote, A. de Roubin, P. Campbell, B. Cheal, C. S. Devlin, T. Eronen, S. Geldhof, I. D. Moore, M. Reponen, S. Rinta-Antila, and M. Schuh, Nucl. Instrum. Methods Phys. Res., Sect. B **463**, 437 (2020).

[40] M. S. Basunia and A. M. Hurst, Nucl. Data Sheets **134**, 1 (2016).

[41] J. M. G. Levins, J. Billowes, P. Campbell, and M. R. Pearson, J. Phys. G **23**, 1145 (1997).

[42] W. Gins, R. de Groote, M. Bissell, C. Granados Buitrago, R. Ferrer, K. Lynch, G. Neyens, and S. Sels, Comput. Phys. Commun. **222**, 286 (2018).

[43] N. Bendali, H. T. Duong, P. Juncar, J. M. S. Jalm, and J. L. Vialle, J. Phys. B **19**, 233 (1986).

[44] A. Klose, K. Minamisono, C. Geppert, N. Frömmgen, M. Hammen, J. Krämer, A. Krieger, C. Levy, P. Mantica, W. Nörtershäuser, and S. Vinnikova, Nucl. Instrum. Methods Phys. Res., Sect. A **678**, 114 (2012).

[45] A. Mueller, F. Buchinger, W. Klempt, E. Otten, R. Neugart, C. Ekström, and J. Heinemeier, Nucl. Phys. **A403**, 234 (1983).

[46] J. Krämer, Construction and commissioning of a collinear laser spectroscopy setup at TRIGA Mainz and laser spectroscopy of magnesium isotopes at ISOLDE (CERN), Ph.D. thesis, Johannes Gutenberg-Universität Mainz, Mainz, 2010.

[47] A. Krieger, C. Geppert, R. Catherall, F. Hochschulz, J. Krämer, R. Neugart, S. Rosendahl, J. Schipper, E. Siesling, C. Weinheimer, D. T. Yordanov, and W. Nörtershäuser, Nucl. Instrum. Methods Phys. Res., Sect. A **632**, 23 (2011).

[48] S. Lechner, Laser spectroscopy of antimony isotopes and the design of a cryogenic Paul Trap, Ph.D. thesis, Technische Universität Wien, Wien, 2021.

[49] V. Batteiger, S. Knünz, M. Herrmann, G. Saathoff, H. A. Schüssler, B. Bernhardt, T. Wilken, R. Holzwarth, T. W. Hänsch, and T. Udem, Phys. Rev. A **80**, 022503 (2009).

[50] A. M. Martensson-Pendrill, L. Pendrill, A. Salomonson, A. Ynnerman, and H. Warston, J. Phys. B **23**, 1749 (1990).

[51] S. Sturm, F. Köhler, J. Zatorski, A. Wagner, Z. Harman, G. Werth, W. Quint, C. H. Keitel, and K. Blaum, Nature (London) **506**, 467 (2014).

[52] W. Huang, M. Wang, F. Kondev, G. Audi, and S. Naimi, Chin. Phys. C **45**, 030002 (2021).

[53] P. Alkemade, C. Alderliesten, P. De Wit, and C. Van der Leun, Nucl. Instrum. Methods Phys. Res. **197**, 383 (1982).

[54] L. Filippin, R. Beerwerth, J. Ekman, S. Fritzsche, M. Godefroid, and P. Jönsson, Phys. Rev. A **94**, 062508 (2016).

[55] Based on personal communication with I. S. Towner (2022).

[56] J. C. Hardy and I. S. Towner, Phys. Rev. C **91**, 025501 (2015).

[57] J. Hardy, I. Towner, V. Koslowsky, E. Hagberg, and H. Schmeing, Nucl. Phys. **A509**, 429 (1990).

[58] I. S. Towner and J. C. Hardy, in *Symmetries and Fundamental Interactions in Nuclei* (World Scientific, Singapore, 1995), pp. 183–249.

[59] I. S. Towner and J. C. Hardy, The current status of $V_{ud}$ (1998).

[60] J. C. Hardy and I. S. Towner, Phys. Rev. Lett. **94**, 092502 (2005).

[61] J. C. Hardy and I. S. Towner, Phys. Rev. C **79**, 055502 (2009).

[62] G. Fricke and K. Heilig, *Nuclear Charge Radii* (Springer, Berlin, 2004).

[63] I. Angeli and K. Marinova, Atomic Data Nucl. Data Tables **99**, 69 (2013).